Identification of Oil-Gas Two Phase Flow in a Vertical Pipe using Advanced Measurement Techniques

Lokman A. Abdulkareem
Department of Petroleum Engineering
College of Engineering
University of Zakho
Duhok, Iraq
lokman.abdulkareem@uoz.edu.krd

***Abstract*—The characteristics of flow configuration in pipes are very important in the oil industry due to its role in governing equipment design. In vertical risers, many flow configurations could be observed such as bubbly, slug, churn, and annular flow. In this project, two tomographic techniques have been applied simultaneously to the flow in a vertical riser: the Electrical Capacitance Tomography (ECT) technique and the Capacitance Wire Mesh Sensor (WMS) technique. The employed pipe diameter was 50mm and the superficial studied velocities were 0.06-3.0m/s for gas and 0.06-0.4m/s for oil. Several techniques have been used to analyze the output data of the two tomography techniques such as time series of cross-sectional averaged void fraction, Probability Density Function (PDF), image reconstruction, and liquid hold-up profile. The averaged void fractions were calculated from the output signal of the two measurement techniques and plotted as functions of the superficial velocity of the gas. The flow patterns were identified from the PDF of the averaged void fraction. In addition, it was found that both tomographic techniques are reliable in identifying the flow regimes in pipes.**

Keywords-insert void fraction; electrical capacitance tomography; wire mesh sensor; two phase flow

I. INTRODUCTION

Multiphase flow of gas-liquid mixtures in vertical pipes occurs in industrial equipment and applications such as petroleum industry, boilers, chemical plants, heat transfer equipment with change of phases, nuclear reactor technology, and geothermal energy production. Two phase flow is a challenging subject due to the complexity of the form in which the fluids exist inside the pipes [1]. The prediction of occurring characteristics such as liquid hold up and gas void friction during the two phase gas/liquid flow in pipes is of particular interest to the nuclear, petroleum, and chemical industries. In some petroleum industry units, obtaining accurate inflow performance relations is difficult due to its multiphase behavior [2]. The most important parameters in multiphase flow are flow regimes and void fraction [3]. Therefore, the understanding of any process in multi-phase flows depends on the identification of flow regimes. As a result, identification of flow regimes is an excellent start for developing techniques that predict gas and liquid hold up, mass and heat transfer, and finally pressure drop. Therefore, the main aim of this study is the characterization of two-phase flow in vertical pipes.

II. EXPERIMENTAL ARRANGEMENT

The study of multi-phase gas-liquid flow requires accurate measurements of each phase velocity and phase fraction. The experimental facilities and equipment setup used in this study are described in [3] and shown in Figure 1. The project measurement technique that has been installed and used on the vertical facility technique is the novel embracing Capacitance Wire Mesh sensor (WMS) [4]. This device is designed in the Research Center of Helmholtz Centrum Dresden Rossendorf (HZDR), Germany.

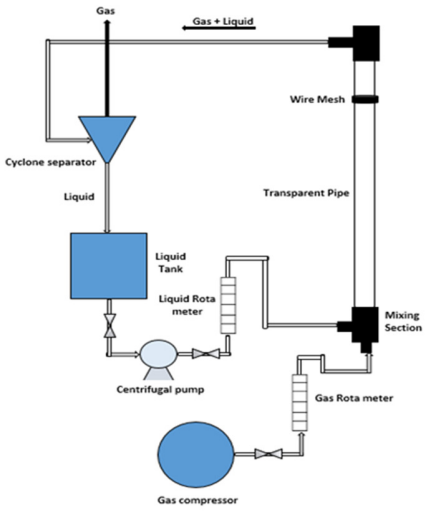

Fig. 1. Block diagram of the facility.

III. PROBABILITY DENSITY FUNCTION

The probability density function (PDF) of the void fraction time series has been used to classify the various flow patterns

Corresponding author: Lokman A Abdulkareem

observed in our previously performed experiments [5]. Typical examples for bubbly, slug, and churn patterns are given in Figure 2. This data corresponds to a liquid superficial velocity of 0.06m/s and gas superficial velocities of 0.06-5.33m/s respectively. The slug flow regime is characterized by twin peaks corresponding to the liquid slug and the Taylor bubble. A single peak existing at a low void fraction is typical of bubbly flow. The PDFs of the conditions of flow rate of oil Uls=0.06 and 0.4m/s and gas superficial velocity of 0.06-5.33 m/s are illustrated on 3 dimensional graphs in Figure 3.

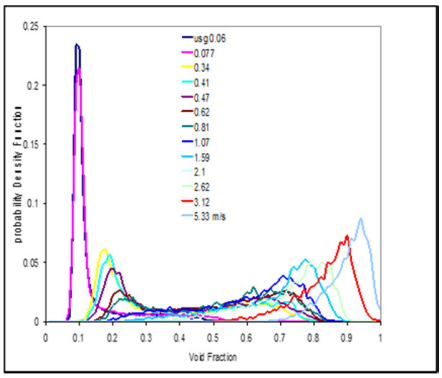

Fig. 2. Probability density function versus gas superficial velocity.

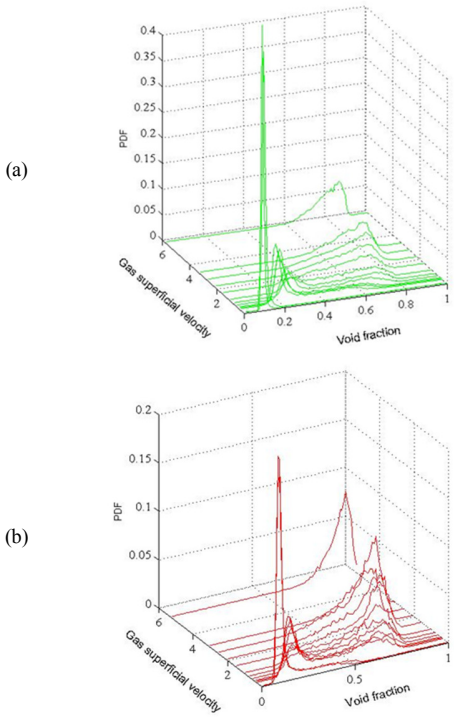

Fig. 3. The PDFs from: (a) Electrical capacitance tomography and (b) wire mesh sensor.

The PDF at the lowest gas flow rate shows a single peak at low void fraction, typical of bubbly or homogeneous flow. As the gas velocity increases, this first peak moves to higher void fractions. In addition, a second peak at a much higher void fraction begins to grow. This second peak is typical of slug flow and represents the emergence of Taylor bubbles. For slug flow, the results from electrical capacitance tomography sensor show a clearer peak than those of wire-mesh sensors. The axial gap between the electrodes is 2mm for wire-mesh sensor, therefore the wire-mesh sensors measure almost instant void fraction at a plane, whilst electrical capacitance tomography probes measure average void fraction over the 13 zones.

IV. MEAN VOID FRACTION

The mean void fraction of two probes for vertical flow has been plotted against the superficial gas velocity in Figure 4. The measurements were conducted under liquid velocity of 0.06m/s and different gas rates. As can be seen from Figure 4, at low gas rates, there is a good agreement between the two curves. However, after the gas superficial velocity reached 1.4m/s, the mean void fraction curve in ECT probe has moved higher than the WMS curve.

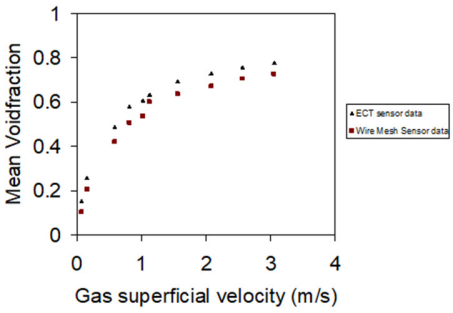

Fig. 4. Mean void fraction of two probes vs. superficial gas velocity.

V. VOID FRACTION PROFILE

The wire-mesh sensor measuring system provides time and cross-sectional resolved information about the spatial distribution of phases. The information can be used to obtain many parameters such as space and time averaged void fractions, radial profiles of time averaged void fraction, and cross-sectional averaged time series of void fraction in the pipe. Time averaged resolved radial gas void fraction profiles were examined for various gas and liquid superficial velocity values. Figure 5 shows the curve shapes of oil-air flow. All peak values are located in the pipe center and increase with increasing gas superficial velocity. These curve shapes are developed by the appearing of relatively large gaseous structures located in the pipe center. This is expected as the flow rates fall in the center peak region [6].

VI. TIME SERIES OF CROSS-SECTIONAL AVERAGED VOID FRACTION

Time series is a calculation method that is used as adjunct to identify and analyze the types of flow pattern inside a vertical pipe. The WMS provides time and cross-sectional resolved information about the spatial distribution of the phases. The time series of cross-sectional average void fraction allows detecting essential features of the flow [7]. Effectively, the time series data show the variation of void fraction with time for each performed run which detects the time each bubble passes through the sensors and is transferred to the output device which in turn records the time taken for each bubble.

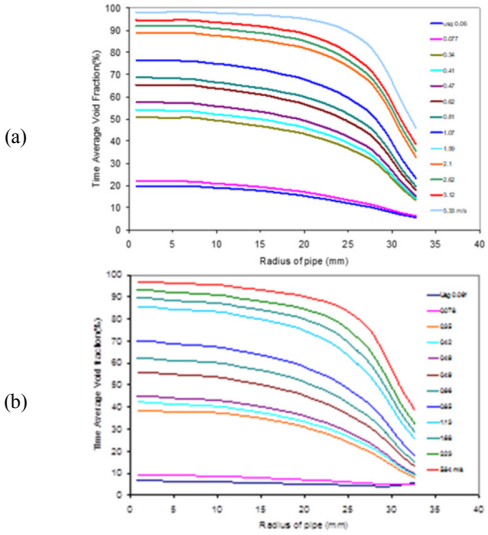

Fig. 5. Radial, time-averaged void fraction profiles for different gas superficial velocities and (a) 0.06m/s, (b) 0.4m/s liquid superficial velocity.

Examples of time series of cross-sectional average void fraction obtained from WMS tomography technique are shown in Figure 6 which explains the difference between bubble size and the amount of gas-liquid inside the pipe. However, the time series method of measurements by itself is not sufficient for identifying the types of flow pattern. Other parameter methods are needed, such as PDF, frequency and mean void fraction techniques. With the presence of these parameters, the detection of flow pattern type is more accurate. The flow pattern types for vertical pipe are bubbly flow, cup bubble flow, slug flow, and churn flow.

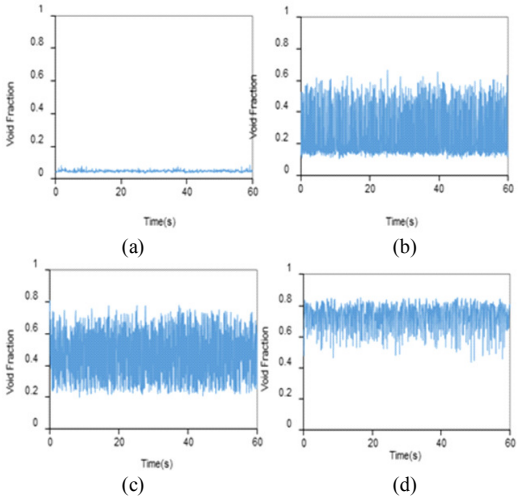

Fig. 6. Time series of cross-sectional average void fraction for (a) bubbly flow, (b) cup bubble, (c) slug flow, and (d) churn flow.

VII. IMAGE RECONSTRUCTION

Electrical Capacitance Tomography (ECT) produces images of permittivity distribution of the mixture of two fluids inside pipes. The permittivity distribution is displayed as a series of normalized pixels located on a 32×32 square pixel grid using an appropriate color scale of graduated blue/green/red to indicate the normalized pixels permittivity [8]. The pixel values corresponding to the lower permittivity material used in the calibration of the sensor have zero value and are displayed in blue whereas pixels corresponding to the higher permittivity material have the value of 1 and are displayed in red. The normalized permittivity distribution corresponds to the fractional concentration distribution of the higher permittivity material. The method which has been used for reconstruction images is known as Linear Back Projection (LBP) and is based on a set of forward and inverse transforms. Several slice images of reconstruction data have been constructed for captured data. Figure 7 shows examples of reconstruction of tomographic images for different superficial oil and gas velocities. The images from the Figure are in agreement with the visual observations. The images in Figure 8 show the transition of a few different flow regimes processed with both visualization techniques.

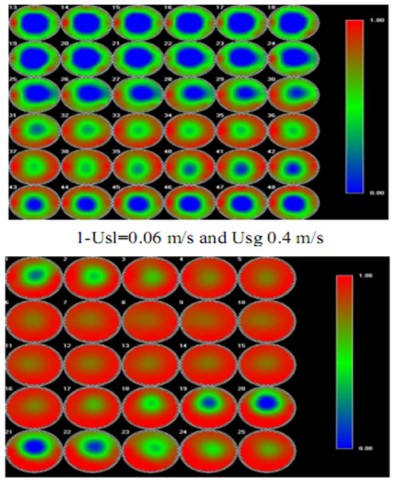

Fig. 7. Tomographic images for flow for different velocitird of liquid and gas.

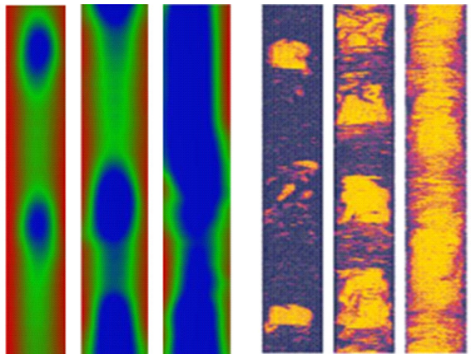

Fig. 8. Visualization of (a) electrical capacitance tomography and (b) wire-mesh sensor data.

It has been experimentally observed that bubbles start forming up at low flow rates. Gradual slug flow occurs due to the increase in the superficial velocity. With further increase in

velocity, the pattern progresses, into churn flow with moderate to high turbulence. Preliminary results obtained using this technique have proved the ECT system as a powerful tool for exploring transient multiphase phenomena in gas–liquid [9].

VIII. THREE DIMENSION PLOTS

Two and three dimension plots of surface contours of the permittivity of the material inside the pipe have been generated by the ECT system. The PLOT3D software allows the capacitance data to be captured and the PTL ECT32 software to be displayed as a set of multiple 2-D image frames and to be viewed in 2 or 3D. The 3D plotting extends the flow visualization of the structure of the flow into the third dimension axially along the pipe. It does this by projecting the structures axially based on the velocity as they pass through the sensor planes. Figure 9 shows an example of 3D data captured by the ECT sensor.

Fig. 9. 3D plot of liquid concentration.

The Wire Mesh Sensors (WMSs) employed in this study are capable of providing the Taylor bubble shapes by creating a 3D reconstruction of the flow as shown in Figure 10. The deformation of a Taylor bubble is also related to the stresses generated from the translational motion. As a result, as the mixture velocity increases it can be observed that the Taylor bubble is totally broken when the gas superficial velocity reaches 1.4m/s. This phase interaction mechanism might be the reason why, as reported in [10], liquid structures inside the gas core of the Taylor bubble (wisps) have been found to exist in the churn flow regime.

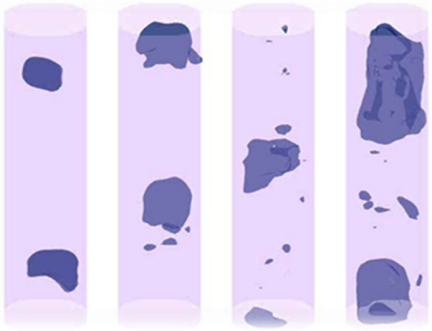

Fig. 10. Taylor bubble shapes in 3D.

IX. LIQUID HOLD UP PROFILE

ECT is a system which processes capacitance data captured by a twin plane ECT sensor to produce velocity and flow profiles and overall flow data for a mixture of 2 dielectric materials. It generates instantaneous concentration (hold up) profiles of the flow inside the ECT sensor, at two axial measurement locations (planes) for each frame of capacitance data. These concentration profiles can be calculated for a relatively small number of zones in the flow cross-section. Figure 11 shows the average concentration (expressed as a percentage of the zone when full, in the nominal range 0-100%) for the selected zone at each of the two measurement planes as a function of time. The Green trace corresponds to the average zone concentration at Plane 1 and the Red trace corresponds to the average zone concentration at Plane 2. Cross-correlation techniques can then be used to derive the instantaneous velocity in each zone from the concentration profiles at the 2 measurement planes. The overall flow profile can also be calculated from the concentration and velocity profiles.

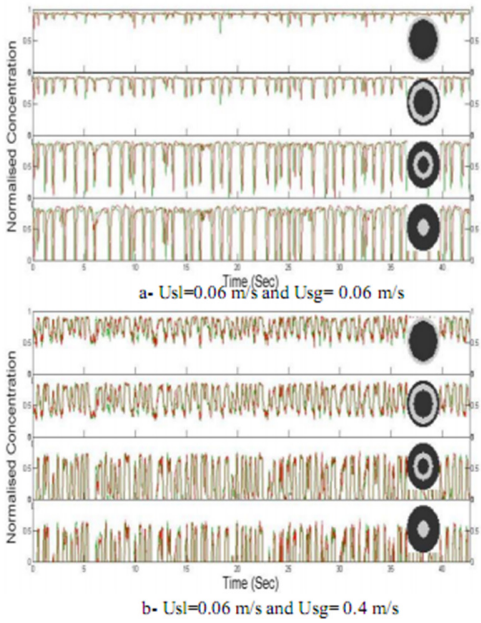

Fig. 11. Time variation of liquid hold up in four marked zones from the two probes.

X. STRUCTURE VELOCITY

Structure velocities have been calculated from the cross correlation of the two void fraction signals from two planes of the ECT sensor. The transient time between the two planes was measured and divided by the distance between the two planes. Figure 12 shows the variation of structure velocity against mixture velocity for all conditions for vertical flow. In addition, the experimental data have been compared with the Nicklin equation. The dash line curve in the Figure is the correlation proposed by [11]. It shows that increasing the mixture velocity leads to increasing in structure velocity. However, at liquid rate of 0.06m/s and gas rate of 1.9m/s, the structure velocity starts to decrease. The reason of this case is the change in flow

pattern from slug to churn. In addition, the experimental structure velocity is higher than the Nicklin curve.

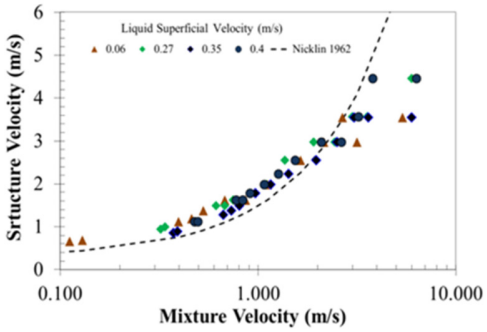

Fig. 12. Structure velocity vs. mixture velocity of gas, for different liquid flow rates.

XI. FREQUENCY ANALYSIS

Frequency analysis is a very important technique on the predication of slug flow characteristics. Accurate designing of separation in two phase flow depends on the reliable predication of slug frequency. The frequency of the data can be found by Power Spectrum Density (PSD) analysis. PSD shows how the power of a signal or time series is distributed with frequency. Mathematically, according to the Wiener-Khinthine theorem, the PSD has been obtained by using Fast Fourier Transform (FFT) of auto covariance function and auto correlation of time series signal. The auto covariance function of a signal $x(t)$ is given by:

$$R_{xx}(\Delta t) = \frac{1}{N}\sum_{t=1}^{N}[x(t)-\bar{x}]\cdot[x(t+\Delta t)-\bar{x}] \quad (1)$$

where $\bar{x} = \frac{1}{N}\sum_{t=1}^{N}x(t)$.

The PSD is then obtained from:

$$P_{xx}(f) = \frac{1}{N}\left(\sum_{t=0}^{N=1}R_{xx}(t)\exp(i2\pi f\tau)\right)2 \quad (2)$$

The autocorrelations for one run are shown in Figure 13. As can be seen, in auto covariance function and FFT there is a single dominant peak which is about 1.2Hz.

Figure 14 shows the effect of gas flow rate on frequency. As can be seen there are break points at bubbly flow to slug and slug to churn transition. The frequency slightly increased with increasing gas flow rate until velocity reached about 0.5m/s and then the frequency starts to decrease due to change in flow regimes from bubbly to slug flow. However, the frequency slightly decreases in slug flow region for higher gas flow rates.

XII. DISCUSSION

This section concentrates on the discussion of the results obtained in the previous sections. Also, the results of the present study are compared with the results obtained in [13].

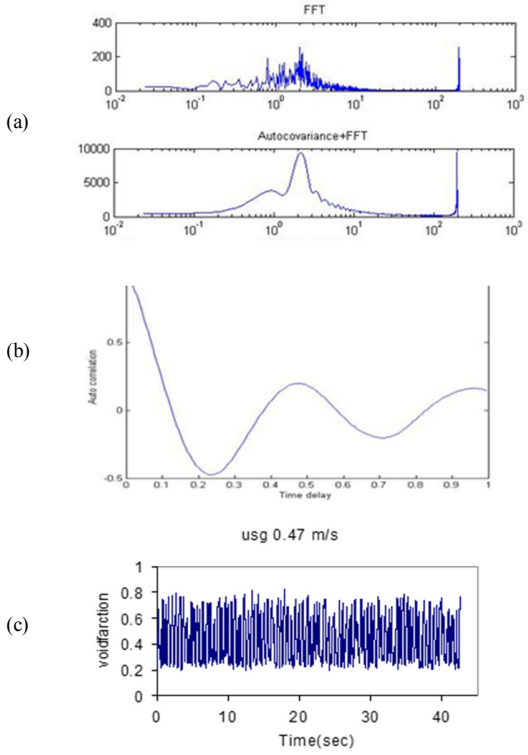

Fig. 13. (a) PSD vs. frequency, (b) auto correlation vs. time delay, (c) time series of void fraction for Usg=0.4m/s and Usl=0.27m/s.

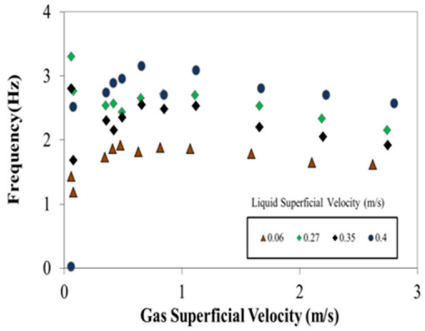

Fig. 14. Frequency against superficial velocity of gas, for different liquid rate flows.

A. Average Void Fraction Analysis

In Figure 15, the variation of average void fraction with gas superficial velocity is shown. The behavior in present work is compared with the results obtained in [13] with silicone oil in pipes of the same diameter. I can be seen that the results follow a comparable trend. Minor differences can be explained by the difference in electrode configurations which brings about a time delay.

B. Probability Density Function

The PDF obtained from the void fraction time series suggested that the flow was bubbly, slug, and churn. The results observed in the present study have been compared with the results obtained in [13]. Three velocities were used for

comparison (Figures 16-18). It can be clearly seen that the PDFs obtained for both studies are of similar character.

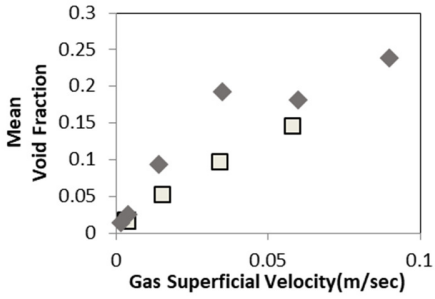

Fig. 15. Result comparison between the current study and [13].

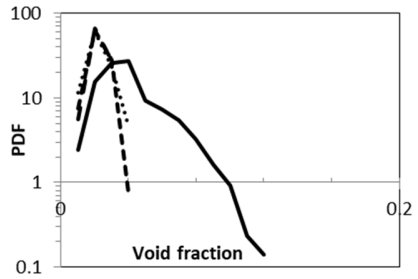

Fig. 16. Current study and [13] comparison of PDFs at 0.003m/s.

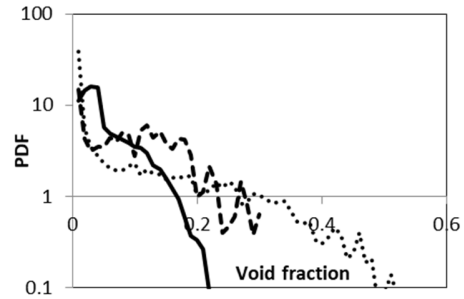

Fig. 17. Current study and [13] comparison of PDFs at 0.001m/s.

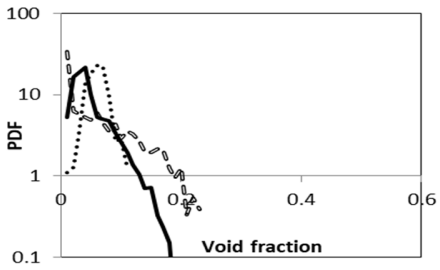

Fig. 18. Current study and [13] comparison of PDFs at 0.02m/s.

C. Dominant Frequency Analysis

The variation of dominant frequencies with gas superficial velocity was compared to the pattern obtained in [13]. The comparison is shown in Figure 19. The plot trend obtained in the present study was found to be significantly different from that obtained in [13]. Here the frequency was found to fluctuate with superficial gas velocity unlike the one obtained in [13]. This fluctuation in frequency value is mainly due to disturbances caused by noise.

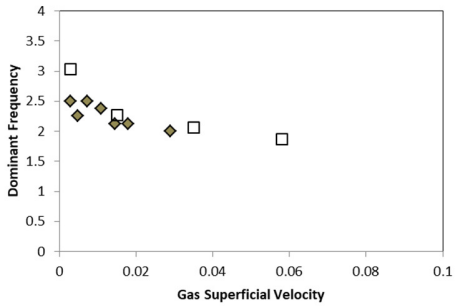

Fig. 19. Comparison of dominant frequencies.

D. Structure Velocity

The structure velocity was found to vary linearly with the gas superficial velocity as shown in Figure 20, implying the flow inside the tube to be slug. The bubble velocities obtained in the present study were compared with the bones obtained in [13] and it was seen that their magnitudes are very similar. This suggests that the bubble behaviors of both liquids can be considered to be similar.

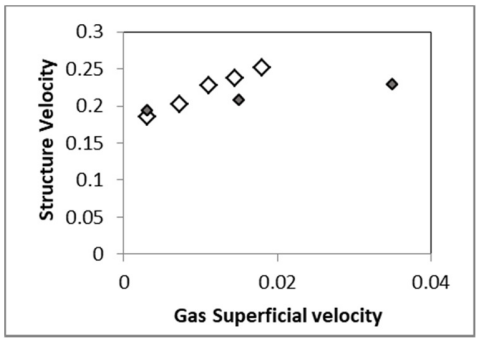

Fig. 20. Comparison of structure velocity.

XIII. CONCLUSION

Two advanced instrumentations were used to examine and investigate the characteristics of two-phase flow in vertical pipes. Experiments were performed in a mixture of gas and oil, revealing good agreement in the flow pattern behavior with similar studies. The ECT has the capability to measure velocity non-intrusively, and is able to show detailed void fraction and velocity profile information for flows. The 3D shape of the bubble was reconstructed from WMS and ECT data. The structure velocity shows similar trends when compared with [11]. PDFs used as in [5] have been used to identify the flow patterns.

ACKNOWLEDGMENT

The author would like to thank the Multiphase Flow Research Center in the Department of Petroleum Engineering, College of Engineering, University of Zakho for funding and supporting this research project.

REFERENCES

[1] B. J. Azzopardi, *Gas-liquid Flows*. New York, NY, USA: Begell House, 2006.

[2] M. H. Chachar, S. A. Jokhio, A. H. Tunio, and H. A. Qureshi, "Establishing IPR in Gas-Condensate Reservoir: An Alternative Approach," *Engineering, Technology & Applied Science Research*, vol. 9, no. 6, pp. 5011–5015, Dec. 2019.

[3] L. A. AbdulKareem, B. J. Azzopardi, S. Thiele, A. Hunt, and M. J. Da Silva, "Interrogation of Gas/Oil Flow in a Vertical Using Two Tomographic Techniques," presented at the ASME 2009 28th International Conference on Ocean, Offshore and Arctic Engineering, Feb. 2010, pp. 559–566, doi: 10.1115/OMAE2009-79840.

[4] V. A. Musa, L. A. Abdulkareem, and O. M. Ali, "Experimental Study of the Two-Phase Flow Patterns of Air-Water Mixture at Vertical Bend Inlet and Outlet," *Engineering, Technology & Applied Science Research*, vol. 9, no. 5, pp. 4649–4653, Oct. 2019.

[5] M. J. Da Silva, S. Thiele, L. Abdulkareem, B. J. Azzopardi, and U. Hampel, "High-resolution gas–oil two-phase flow visualization with a capacitance wire-mesh sensor," *Flow Measurement and Instrumentation*, vol. 21, no. 3, pp. 191–197, Sep. 2010, doi: 10.1016/j.flowmeasinst.2009.12.003.

[6] G. Costigan and P. B. Whalley, "Slug flow regime identification from dynamic void fraction measurements in vertical air-water flows," *International Journal of Multiphase Flow*, vol. 23, no. 2, pp. 263–282, Apr. 1997, doi: 10.1016/S0301-9322(96)00050-X.

[7] Ohnuki A. and H. Akimoto, "Experimental Study on Transition of Flow Pattern and Phase Distribution in upward air-water Two-phase Flow along a Large Vertical Pipe", International Journal of Multiphase Flow, Vo. 26, pp 367-386, 2000.

[8] M. Abdulkadir, D. Zhao, S. Sharaf, L. Abdulkareem, I. S. Lowndes, and B. J. Azzopardi, "Interrogating the effect of 90° bends on air–silicone oil flows using advanced instrumentation," *Chemical Engineering Science*, vol. 66, no. 11, pp. 2453–2467, Jun. 2011, doi: 10.1016/j.ces.2011.03.006.

[9] M. Byars, "Developments in electrical capacitance tomography," *2nd World Congress on Industrial Process Tomography*, pp. 542–549, Jan. 2014.

[10] W. Warsito and L.-S. Fan, "Measurement of real-time flow structures in gas–liquid and gas–liquid–solid flow systems using electrical capacitance tomography (ECT)," *Chemical Engineering Science*, vol. 56, no. 21, pp. 6455–6462, Nov. 2001, doi: 10.1016/S0009-2509(01)00234-2.

[11] B. Azzopardi, V. Hernandez Perez, R. Kaji, M. J. Da Silva, M. Beyer, and U. Hampel, "Wire mesh sensor studies in a vertical pipe," in *Proceedings of the 5th International Conference on Transport Phenomena in Multiphase Systems, HEAT 2008*, Bialystok, Poland, 06.-03.07 2008.

[12] E. Q. Bashforth, J. B. P. Fraser, H. P. Hutchison, and R. M. Nedderman, "Two-phase flow in a vertical tube," *Chemical Engineering Science*, vol. 18, no. 1, pp. 41–46, Jan. 1963, doi: 10.1016/0009-2509(63)80004-4.

[13] M. M. Mustafa, "Investigation of Gas-Liquid Flow in Vertical Pipes by using Wire-Mesh Sensor & Measuring the Viscosity Flow of Fluids using BS/U/M Viscometers," Ph.D. dissertation, University of Zakho, Zakho, Iraq, 2013.